JOURNAL OF PROPULSION AND POWER
Vol. 16, No. 6, November–December 2000

Three-Dimensional Automatic Optimization Method for Turbomachinery Blade Design

K. F. C. Yiu* and M. Zangeneh†
University College London, London, England WC1E 7JE, United Kingdom

In deriving automatic numerical optimization algorithms for aerodynamic applications, it is quite important to choose a suitable cost function and a suitable set of design parameters. The unknown airfoil/blade profiles are usually chosen to be the design parameters. However, there are certain advantages in using the pressure/velocity distribution as the design variable in some applications; the optimized distribution can be used in a three-dimensional inverse design method to generate the actual profile shape. In this paper this approach will be addressed. Two methods are used to parameterize the circulation distribution for compressor blades. The Dawes code is used to calculate the viscous effect. An automatic optimization algorithm is developed, and two objective functions defined by the entropy loss or the aerodynamic blockage are examined.

Nomenclature

C_p	=	specific heat
M	=	Mach number
$Mu2$	=	Mach number based on stagnation temperature and impeller tip speed
m	=	meridional coordinate
N_b	=	number of blades
p^+, p^-	=	pressure on the upper and lower surface of blade
R	=	gas constant
$r\bar{v}_\theta$	=	circulation distribution
S	=	entropy
W_{bl}	=	relative velocity on blade surface

I. Introduction

SINCE the development of computational fluid dynamics (CFD), a lot of efforts have been devoted to the derivation of automated methodology. The general objectives that such efforts are trying to accomplish are to decrease human involvement in the search for improved designs; it is hoped that designers will have better tools than the use of cut-and-try approaches.

One popular approach to introduce automatic algorithms is to use numerical optimization methods. The design problem is formulated as a constrained optimization problem so that standard techniques, such as the gradient methods, can be applied. To formulate the design problem, first of all, a suitable cost function is required. Second, suitable design variables are required to give maximum design flexibility with the lowest dimensions. Third, a reliable flow solver that gives accurate flowfield prediction for a wide range of variations in the design parameters is required. Fourth, practical optimization algorithms are required to solve the problem within a reasonable time limit. These issues will be addressed here for the design of centrifugal compressor impeller blades.

In the design of impeller blades, it is often the case that when the flow is separated, the off-design performance is very poor. Because the efficiency of the turbomachine should decrease when the flow is separated, it is therefore natural to choose to minimize the loss, which is a good measure of efficiency. Another good measure is the blockage that usually decreases significantly at the separated region; therefore, the maximum blockage along the chord is another good indicator of a poor flowfield. Both the loss and the blockage are examined here in the optimization formulation.

Received 5 April 1999; revision received 2 September 1999; accepted for publication 2 September 1999.

*Senior Lecturer, Department of Mechanical Engineering.
†Research Fellow, Department of Mechanical Engineering.

For the design variables one way is to parameterize the unknown shape directly. The first attempt is to restrict the changes to a relatively small number of smooth geometric modes and add to the original profile shape as perturbations. This approach has been applied by Refs. 1 and 2. Gradually, the use of spline functions to represent the profile geometry directly has gained popularity because of their smoothness and flexibility in making localized modifications. Using the compact support property, the designers can modify the geometry in certain important regions only while keeping a smooth curvature variation for the rest of the profile. In this way the dimension of the problem is greatly reduced, which makes three-dimensional optimization designs possible. This approach has been applied by the authors in Refs. 3 and 4 for two-dimensional designs and by the authors in Refs. 5 and 6 for three-dimensional designs.

Another way to define the design variables is to parameterize the velocity distribution instead and solve for the blade by using an inverse method. This approach was first explored by the authors in Refs. 7 and 8, who parameterized the pressure distributions for two-dimensional airfoil sections based on the flow characteristics in different sections. Several successful inverse methods have been developed today, such as in Refs. 9–11, in which a target pressure/velocity distribution is imposed as a boundary condition to the partial differential equations. Traditionally, designers need to guess a good target distribution based on experiences and input to the inverse method. However, if the distribution is parameterized and used as the design variables in an optimization context, the optimal distribution input to the inverse design method can be sought automatically.

There are several advantages of using the distribution as the design variables instead of the blade shape itself, noticeably that many experienced designers may find it easier to handle the pressure/velocity distributions directly instead of the actual profile geometry because distributions usually give more insight to the problem being solved than the shape itself. In addition, as pointed out by Ref. 7, by judging from the data published in Ref. 12, relatively simple pressure/velocity distribution modifications lead to complicated variations in the profile geometry, which indicates that it may be advantageous to optimize the distribution directly by numerical optimization; this may lead to considerable savings in computations for some cases. A third advantage is that work (and therefore blade loading) can be roughly kept constant throughout the optimization process. Fixing the blade loading is quite important for many applications, but it is very difficult to maintain during the optimization process with profiles being the design variable.[13] However, a constant work constraint can easily be imposed to the target distribution and only those fulfilling the constraint will be generated.

In this paper the design variable is the blade-bound circulation (or swirl velocity) distribution. Two different ways of parameterizing

the distribution are proposed and compared. The first method is based on a three-segment description of the loading distribution used in Ref. 14; the circulation distribution is then sought by integrating the loading distribution. The second method is to represent the circulation distribution directly using a cubic-spline curve bounded by a control polygon. Once the circulation is defined, the inverse method developed by Ref. 11 is used to calculate the blade-wrap-angle distribution and to generate the whole three-dimensional blade geometry. The Dawes code,[15] which solves the full three-dimensional Navier–Stokes equations in the blade-to-blade plane, is evoked to predict the viscous flowfield. Because both the inverse method[11] and the Dawes code have been validated carefully, such as in Refs. 14 and 16, we will concentrate on the application of these two methods here.

After the formulation of the optimization problem, a suitable optimization method is needed. There are various techniques developed today. In general, apart from the techniques being used in mathematical programming, most of the methods are based on search directions such that the objective function decreases along the search direction in each iteration. Methods used to find a suitable search direction can usually be categorized into two types. The first category is the gradient methods or the quasi-Newton methods in which the gradient information is used to define the search directions. The second category is the no-derivative methods in which the search directions are selected based on intuition. Computer costs increase significantly with the number of unknowns for the no-derivative methods. They are therefore useful only when the dimension of the problem is low.

To choose the right method, typical characteristics of the problem are assessed, which include the cost to evaluate the objective function, the cost and the accuracy to acquire the gradient information, the smoothness of the objective function, and the number of unknown parameters in the problem. In general, if the objective function is highly nonsmooth, gradient techniques usually perform poorly because they can easily be trapped by local minimums near to the initial guess. In addition, if objective function evaluations are very expensive computationally, or if the number of unknown parameters is large, the adjoint equation, which can be derived either analytically[17–19] or via automatic differentiations,[20] is required to calculate the gradient information to give a computationally viable method.

In the present application because each evaluation of the objective function requires a solution of the Navier–Stokes equations, it is therefore very expensive to calculate. Also, as the present Navier–Stokes solver is used as a black-box solver, it is very difficult to derive the adjoint equation like Ref. 4. If the gradients are calculated approximately via numerical differentiation, it will be very expensive and may not be accurate enough. This is particularly so here because of the convergence criteria for the Navier–Stokes solver. It is usually sufficient from a practical point of view to achieve a specified mass-flow rate within a certain percentages of fluctuation. But this narrow fluctuations in the solutions will greatly impair the accuracy of numerical differentiations.

Another crucial selection criterion is the number of local minimums, which is expected to be fairly large because of the nonlinearity of the problem. This is particularly so here because some of the unknowns in the three-segment parameterization are integers; such optimization problems are well known to have numerous local minimums, and the objective function is also nondifferentiable. Thus, the gradient methods are not applicable.

Because the dimension of unknown parameters remains fairly low for most of the applications and it has been reported earlier that best results have been obtained using a simple line search method rather than the use of a sophisticated gradient technique, under such circumstances the alternative-variables method[21] and the simplex method[22] are employed here. Both methods are tested and compared.

II. Objective Function

In measuring the performance of a machine, a measure of aerodynamic loss is required. There are different loss coefficient definitions available, such as the stagnation pressure loss coefficient and the enthalpy loss coefficient. However, these blade-row loss coefficients are not directly applicable here because the relative stagnation pressure and the relative stagnation enthalpy can change as a result of changes in radius. Another way to measure loss in an adiabatic machine is the entropy generation. Entropy is a particularly convenient measure because its value does not depend on whether it is viewed from a rotating or a stationary blade row. For a perfect gas the change in specific entropy is calculated as

$$S - S_{\text{ref}} = C_p \log(T/T_{\text{ref}}) - R \log(p/p_{\text{ref}}) \tag{1}$$

where subscript ref denotes quantities at a particular reference point. Using ΔS, the entropy loss coefficient can be defined and calculated. Here, the loss at the trailing edge is used while the reference point is taken to be the inlet.

Another way to measure the performance of the flowfield is blockage. Although the aerodynamic blockage has been widely used for different purposes such as processing of experimental measurements,[23] its use in optimization has not been explored. In external flow over aerofoils, it is usually possible to distinguish between viscous and inviscid regions, and therefore the aerodynamic blockage can be defined using the displacement thickness of the boundary layer. However, this definition is rather difficult for turbomachinery calculations. A more appropriate definition is to use the ratio of the area (pitchwise) averaged meridional velocity to the mass-averaged meridional velocity, written as

$$B_{\text{aero}} = \frac{\bar{V}_m^{\text{area}}}{\bar{V}_m^{\text{mass}}} \tag{2}$$

where

$$\bar{V}_m^{\text{mass}} = \frac{\int_{\text{hub}}^{\text{tip}} \int_{\theta_l}^{\theta_u} \rho V_m V_m r \, \mathrm{d}\theta \, \mathrm{d}n}{\int_{\text{hub}}^{\text{tip}} \int_{\theta_p}^{\theta_s} \rho V_m r \, \mathrm{d}\theta \, \mathrm{d}n} \tag{3}$$

$$\bar{V}_m^{\text{area}} = \frac{\int_{\text{hub}}^{\text{tip}} \int_{\theta_l}^{\theta_u} V_m r \, \mathrm{d}\theta \, \mathrm{d}n}{\int_{\text{hub}}^{\text{tip}} \int_{\theta_l}^{\theta_u} r \, \mathrm{d}\theta \, \mathrm{d}n} \tag{4}$$

For an efficient machine the aerodynamic blockage should be close to one. An aerodynamic blockage close to one indicates uniform flow, which should minimize mixing loss. Notice that blockage varies along the meridional direction and drops significantly when there is a flow separation; a practical indicator for efficiency is therefore

$$1 - \max(B_{\text{aero}}) \tag{5}$$

where max is taken to be between the blade leading edge and trailing edge.

III. Circulation Distribution

The approach applied here is to search for the optimum swirl velocity (denoted by $r\bar{v}_\theta$) distribution at both the hub and shroud and then interpolate linearly between these values to obtain the overall distribution in the meridional plane. This distribution can then be used as the input to the inverse method.[11] At the leading and trailing edges the value of $r\bar{v}_\theta$ is obtained from Euler's pump equation. Furthermore, because the jump in pressure across the blades is given by

$$p^+ - p^- = (2\pi/N_b)(\rho \boldsymbol{W}_{\text{bl}} \cdot \nabla r\bar{v}_\theta) \tag{6}$$

the derivative of $r\bar{v}_\theta$ in the meridional direction must be set to zero at the trailing edge to satisfy the Kutta condition; it is often set to zero as well at the leading edge to fulfill the no-incidence condition.

There are several ways to define the circulation distribution complying with the preceding criteria. As Eq. (6) suggests that the

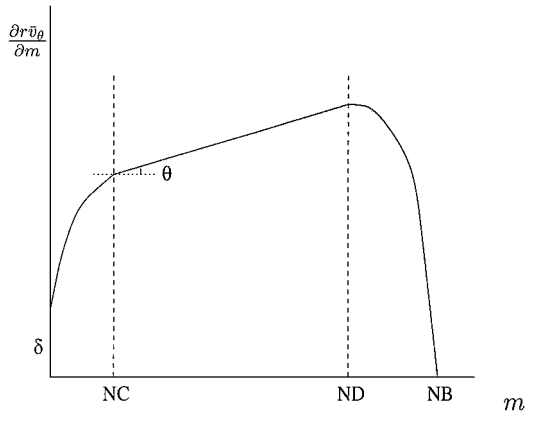

Fig. 1 Three-segment parameterization.

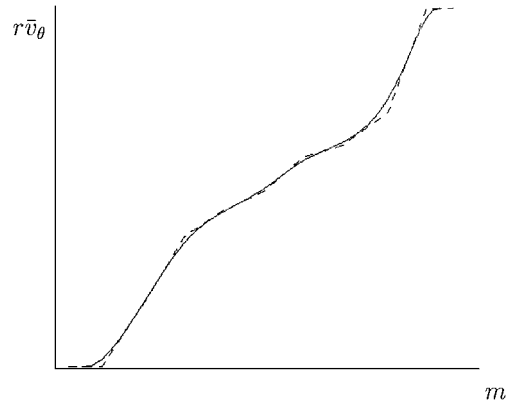

Fig. 2 Spline parameterization.

pressure distribution on the blades is directly related to the loading distribution (meridional derivative of $r\bar{v}_\theta$), the first approach is to use a smooth loading distribution and integrate to get $r\bar{v}_\theta$; this will ensure a smooth pressure distribution. A typical parameterization applied here is depicted in Fig. 1. The distribution is parabolic up to the mesh point NC, then a linear variation between mesh points NC and ND with a specified slope; this is followed by another parabolic segment, which reduces the loading to zero at the trailing edge (mesh point NB) so that the Kutta condition is satisfied. The $\partial r\bar{v}_\theta/\partial m$ distribution is set up in such a way that the area under it is fixed, thereby ensuring fixed specific work design. More details are given in Ref. 14. There are a total of eight parameters that will vary the overall $r\bar{v}_\theta$ distribution, namely (δ_{hub}, θ_{hub}, NC_{hub}, ND_{hub}) and (δ_{tip}, θ_{tip}, NC_{tip}, ND_{tip}). By varying NC and ND and the slope, the loading distribution changes from fore-loaded to evenly loaded and then to rear-loaded easily, which is a fairly comprehensive set. In practice, bounds are imposed on the variables for both the hub and shroud as

$$0 \le \delta \le 2, \qquad -78 \text{ deg} \le \theta \le 78 \text{ deg}$$
$$5 \le NC \le ND \le M - 5 \tag{7}$$

where M is the number of meridional mesh points. In some high-speed applications the impeller is usually designed to have certain positive incidence. Therefore, in this optimization methodology δ is used to change the design point incidence, which can be seen from Eq. (6).

The second way is to represent $r\bar{v}_\theta$ by a cubic B-spline curve, which has continuous first- and second-order derivatives and the variation diminishing property.[24] Using a control polygon with coordinates $\{b_i, i = 0, \ldots, n\}$, the cubic B-spline curve is defined as

$$P(t) = \sum_{i=1}^{n} b_i B_i(t) \tag{8}$$

where $[B_i(t)]$ are the cubic B-spline basis functions with the set of knots

$$\mathcal{N} = (t_0, \ldots, t_n) \tag{9}$$

Because the basis functions have compact local support, changing a point in the corresponding control polygon changes the course of the curve only locally, and the influence of each control point can be pinpointed precisely. It is also possible to introduce additional control points easily; therefore, less control points may be used initially to search for improved designs. In particular, if the set of knots [Eq. (9)] is chosen to be the integer set

$$\mathcal{N} = (0, \ldots, n) \tag{10}$$

Eq. (8) becomes the uniform B-spline curve, which can be simplified to[25]

$$P(t) = \frac{1}{6}\begin{pmatrix} t^3 \\ t^2 \\ t \\ 1 \end{pmatrix}^T \begin{pmatrix} -1 & 3 & -3 & 1 \\ 3 & -6 & 3 & 0 \\ -3 & 0 & 3 & 0 \\ 1 & 4 & 1 & 0 \end{pmatrix} \begin{pmatrix} b_i \\ b_{i+1} \\ b_{i+2} \\ b_{i+3} \end{pmatrix} \tag{11}$$

where $t \in [0, 1]$.

To fix the incidence condition at the leading edge and to satisfy the Kutta condition at the trailing edge, the second and the penultimate control points are fixed to give the required slopes. Because $r\bar{v}_\theta$ is also given at the leading and trailing edge by the Euler's pump equation, two extra control points are used, one at each end extended by an equal distance and slope with the corresponding segment. A typical $r\bar{v}_\theta$ together with its control polygon is shown in Fig. 2. The loading distribution can be sought by differentiating $r\bar{v}_\theta$.

In practice, although the cubic B-spline ensures the continuity and differentiability of the loading distribution, it does not control the number of inflection points in $r\bar{v}_\theta$, and the loading distribution might have excessive numbers of turning points, which in turn gives rise to an impractical blade-wrap-angle distribution. To avoid this, the total curvature of the circulation distribution is controlled via

$$\int_{s_{\text{le}}}^{s_{\text{te}}} |r\bar{v}_\theta{}''(s)|\, \mathrm{d}s < \epsilon_\kappa \tag{12}$$

where ϵ_κ is a predefined constant.

IV. Optimization Algorithms

One of the highly successful methods that requires only function evaluations, not derivatives, is the simplex method proposed by Ref. 22. The method has a very delightful geometrical description. A simplex is the geometrical figure consisting, in N dimensions, of $N + 1$ points (or vertices) and all their interconnections. In two dimensions a simplex is a triangle, whereas it is a tetrahedron in three dimensions. During the searches, the simplex can be either reflected, expanded, or contracted depending on the conditions. More details can be found in Ref. 26.

Another simple but useful method is the alternative-variables method, which the search directions are simply chosen to be

$$\boldsymbol{s}_i = \boldsymbol{e}_i \qquad i = 1, \ldots, n \tag{13}$$

where $\boldsymbol{e}_i$ denote the Cartesian basis vectors and n denotes the number of parameters. Specifically, for $i = 1, \ldots, n$, the point $\boldsymbol{x}^{(k+1)}$ is calculated from $\boldsymbol{x}^{(k)}$ by changing the kth component of $\boldsymbol{x}^{(k)}$ so that

$$L\left[\boldsymbol{x}^{(k+1)}\right] = \min_x L\left[x_1^{(k)}, \ldots, x_{k-1}^{(k)}, x, x_{k+1}^{(k)}, \ldots, x_n^{(k)}\right] \tag{14}$$

Thus, a complete optimization cycle includes n one-dimensional optimizations. Although the method may be inefficient for functions

with second derivatives much larger in magnitude in some directions than in others and has been shown by Ref. 27 to be nonconvergent for some pathological cases with certain starting points or with the same order of searchings in all cycles, it nevertheless performs reasonably well in practice for many functions to give significant decreases in the first few complete cycles and can easily be switched to Powell's direction set method[26] if neccessary.

Because each evaluation of $L(\alpha)$ requires the solution of the Navier–Stokes equations once, it is advantageous to make the best use of the present converged solution as the initial guess. If α changes gradually, the solver of the Navier–Stokes equations can reconverge to a new solution quickly. In view of this, in solving the one-dimensional optimization problem the step size $\alpha^{(k)}$ is increased or decreased gradually by a fixed amount ϵ_α so that

$$L\left[\boldsymbol{x}^{(k+1)}\right] = \min_{\alpha} L\left[\boldsymbol{x}^{(k)} + \alpha \boldsymbol{s}^{(k)}\right] \tag{15}$$

where $\alpha = (\epsilon_\alpha, 2\epsilon_\alpha, \ldots) \cup (-\epsilon_\alpha, -2\epsilon_\alpha, \ldots)$; the search is stopped only either if

$$\left|L\left[\boldsymbol{x}^{(k)} + \alpha^{(k)}\boldsymbol{s}^{(k)}\right] - L\left[\boldsymbol{x}^{(k)}\right]\right| > \epsilon_1 \tag{16}$$

where ϵ_1 is a predefined tolerance, or if the constraint [Eqs. (7) or (12)] is violated. The searches used in Eq. (15) resemble the spirit of the continuation method in solving a system of nonlinear equations when the starting guess is far from the final solution. Moreover, because the search will not be terminated until Eq. (16) or the constraint is violated, a large ϵ_1 will allow $L(\alpha)$ to increase as well as to decrease, and this helps to bypass those local minimums around $\boldsymbol{x}^{(k)}$.

V. Algorithm

In the algorithm the normal thickness distribution corresponding to an original conventional impeller is specified. When the $r\bar{v}_\theta$ distribution is varied during optimization, the meridional geometry, rotational speed, and mass-flow rate are kept constant. The final algorithm can be briefly summarized as follows:

0) Specify an initial $r\bar{v}_\theta$ distribution.

1) Use the inverse design method to generate the blade shape.

2) Use the three-dimensional viscous code to calculate the viscous flowfield and hence predict the loss or the blockage.

3) Modify the $r\bar{v}_\theta$ distribution and goto 1.

From the present algorithm it is clear that the inverse design method is used only as a mapping between the $r\bar{v}_\theta$ distribution and the blade shape. The inviscid flowfield is never used in the optimization process. Once the blade shape is generated, the objective function (either the loss or the blockage) is calculated in step 2 using the three-dimensional viscous code. One way to view this formulation is that the objective function is a nonlinear function of the blade shape defined via the three-dimensional viscous code, whereas the blade shape is another nonlinear function of the $r\bar{v}_\theta$ distribution defined via the inverse design method. As a result, the objective function is a highly nonlinear function of the $r\bar{v}_\theta$ distribution. Under this formulation, the optimization algorithm can be applied to minimize the objective function with respect to the $r\bar{v}_\theta$ distribution. Either the simplex or the alternating-variables method is used in step 3 to optimize the $r\bar{v}_\theta$ distribution.

In using the three-dimensional viscous code in step 2, the exit pressure is specified, and the mass-flow rate is predicted. To achieve a certain mass-flow rate, an additional loop is constructed to iterate on the backpressure until the desired mass-flow rate is reached. The iterations can be summarized as follows:

1) Specify an initial exit pressure and a target mass-flow rate M_f^*.

2) Solve the Navier–Stokes equations for the mass-flow rate M_f via time steppings. The iterations stop if either a maximum number of iterations is reached or the loss converges to satisfy $|L^{(t+T)} - L^{(t)}| < \epsilon_t$ (a constant), where T is a predefined number of time steps.

3) If $|M_f - M_f^*| > \epsilon_m$ (a constant), update the exit pressure via secant iterations and goto 2.

The choice of the tolerance ϵ_m on the mass-flow rate convergence was studied very carefully by testing the optimization algorithm on a similar but slower speed problem with different tolerant values. It turns out that ϵ_m can be increased to about $\pm 10\%$ of the target mass-flow rate without affecting the optimization results. It is therefore a practical choice during optimization searches, both giving accurate loss predictions and avoiding excessive iterations in the Navier–Stokes solver.

VI. Application of Optimization Methods

The algorithm was applied to the design of two generic high specific speed industrial centrifugal compressors. An initial blade is chosen, which has performance of the same level as a state-of-art compressor impeller. Viscous calculations were mostly performed on meshes have a nonuniform pitchwise and spanwise mesh spacing clustering toward the blades. The mesh size is chosen based on previous experiences in the study of the three-dimensional viscous code.[14,16] Because the impeller is shrouded, tip leakage effects were not modelled. The $r\bar{v}_\theta$ is nondimensionalized by the tip speed and the tip radius. The design conditions for the first impeller are as follows: number of blades, 17; tip diameter, 0.5 m; rotational speed, 13,369 rpm; mass-flow rate, 12.5 kg/s; exit axial width, 0.0424 m; and exit tangential velocity, 240 m/s.

The design conditions for the second impeller are as follows: number of blades, 20; tip diameter, 0.28 m; rotational speed, 21,000 rpm; mass-flow rate, 2.25 kg/s; exit axial width, 0.017 m; and exit tangential velocity, 200 m/s.

In the following, the first impeller is applied for various comparison studies. Unless specified otherwise, the alternating-variables method was applied.

A. Effect of Objective Functions

First of all, it is of interest to know whether loss minimization and 1—max(blockage) minimization will yield the same optimal solution starting from the same initial guess. Because the three-segment parameterization contains integer variables, this is a more stringent test for comparison study and is therefore used here. Only one complete cycle was executed so that the one-dimensional minimization [Eq. (15)] was executed once for each variable. From the convergence history of the loss and blockage minimization (Fig. 3), a high correlation is shown, which is a sign that the converged solution should agree reasonably well with each others. As seen from Fig. 4, both loading distributions are rear loaded. At the leading edge of the hub distribution, the discrepancy is high, but a careful examination into the blockage variation during the optimization process reveals that it is purely a numerical effect because the changes in blockage are trivial when the hub loading at the leading edge is varied from 0 to 0.75. The initial and final velocity vectors as predicted by the viscous code near the suction side are shown in Figs. 5 and 6, respectively. Clearly the separation has been eliminated by the algorithm. Because the velocity vectors are extremely close for both

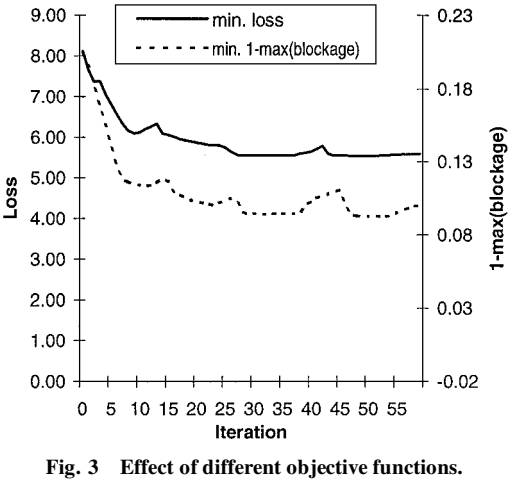

Fig. 3 Effect of different objective functions.

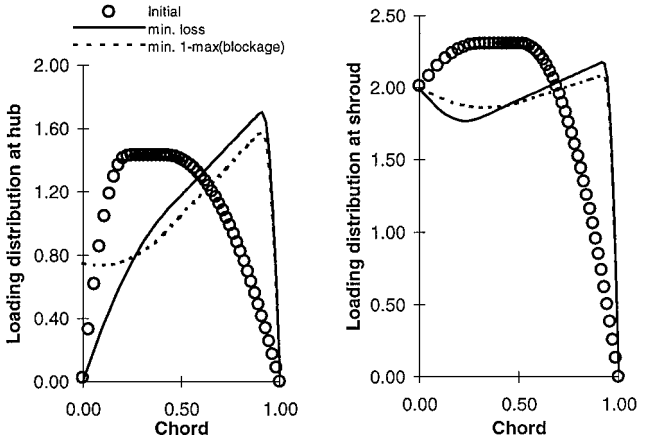

Fig. 4 Comparison of loading distribution.

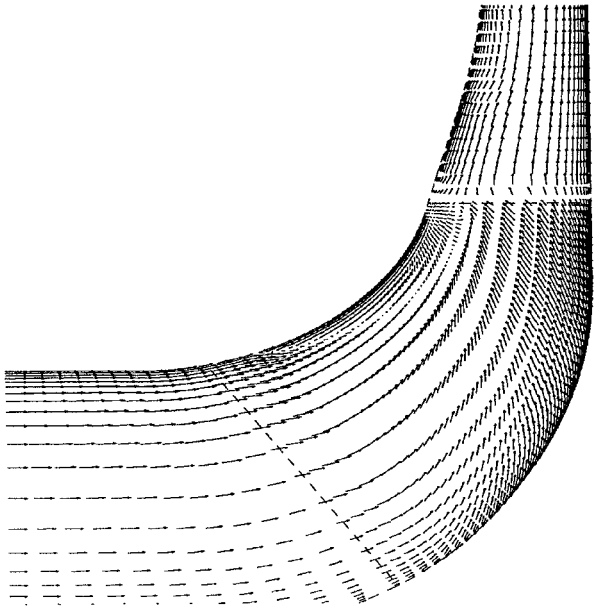

Fig. 5 Initial suction-side velocity vectors.

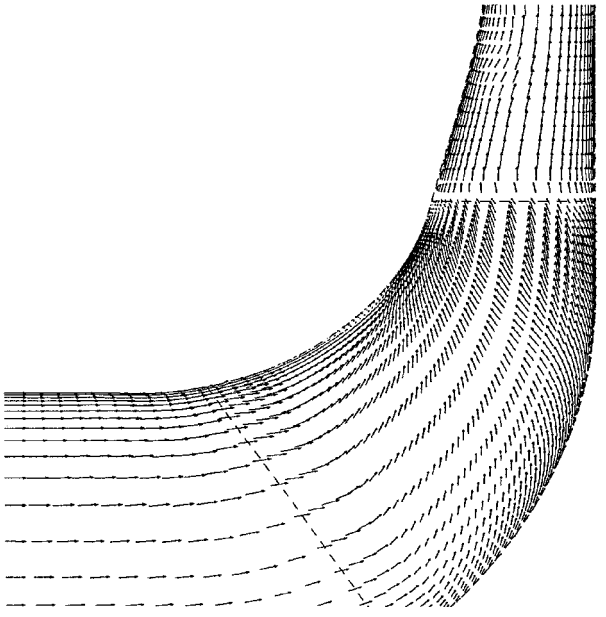

Fig. 6 Optimized suction-side velocity vectors.

minimizations, only the result from the loss minimization is used in Fig. 6. From this comparison study we can conclude that both objective functions are effective in reducing separation and hence improving efficiency. Also, for this test case the optimized result is not sensitive to the hub loading movements at the leading edge.

B. Effect of Mesh Sizes

Second, it is of interest to know whether the optimization process is mesh dependent, which is very important because the algorithm converges a lot faster on a coarser mesh. We expect that when the coarse grid has predicted the flowfield approximately the algorithm should converge to the same solution. This is confirmed by Fig. 7, which shows that the convergence history is reasonably correlated when loss minimization is executed and the converged loading distributions agree closely. Here, the coarse grid contains $17 \times 81 \times 17$ mesh points, and the fine grid contains $25 \times 81 \times 25$ mesh points. Note that the loss predicted by both coarse and fine meshes are closer when the separation has been eliminated. From this comparison study we can conclude that the optimized result is not sensitive to mesh dimensions, as long as the essential feature of the flowfield has been captured in the calculations.

C. Effect of Design Parameterizations

When the B-spline parameterization is used in loss minimization instead, the convergence history is shown in Fig. 8. Three control points were used, and the viscous calculations were on a $17 \times 81 \times 17$ mesh. The level of minimum loss achieved is similar to the result of using the three-segment parameterization; however, from Fig. 9 the loading distribution is more rear loaded at the hub. Figure 9 clearly demonstrates the flexibility a spline curve can achieve comparing with the three-segment technique. The velocity vectors at the suction side are very similar to Fig. 6 and are not reproduced here. The off-design performance of this result is assessed for different mass-flow rates using the viscous code. The results are shown in Fig. 10. Clearly, there is quite a reasonable range of mass-flow rates with efficiency greater than 94% for the

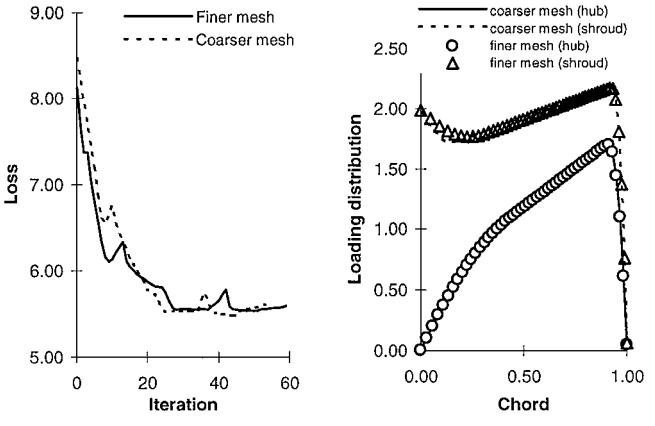

Fig. 7 Effect of different mesh sizes.

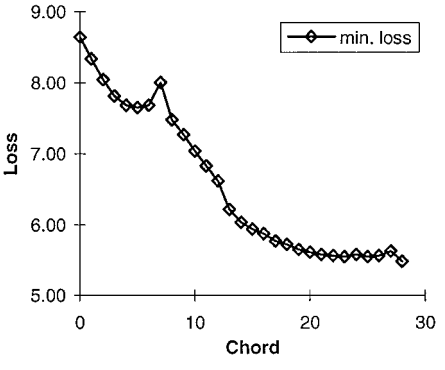

Fig. 8 Convergence history of the spline optimization.

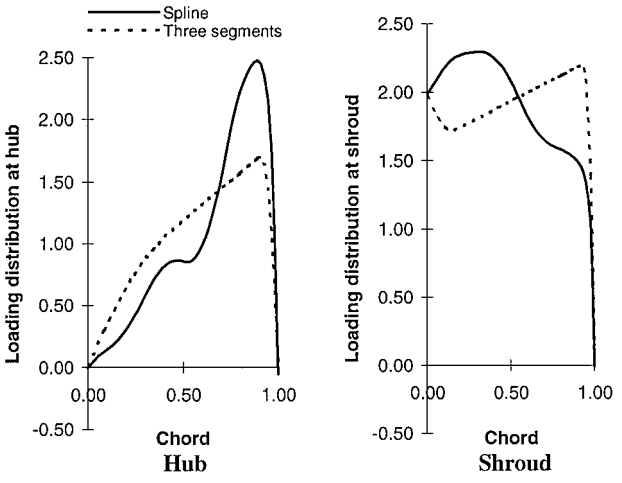

Fig. 9 Comparison of the optimized loading distribution.

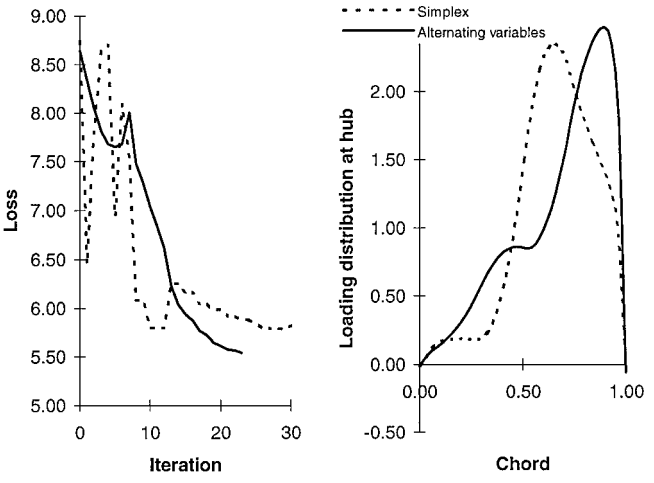

Fig. 12 Comparison of different optimization techniques.

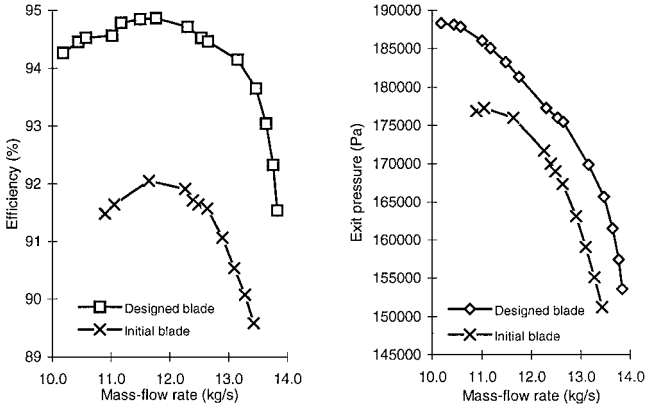

Fig. 10 Off-design performance.

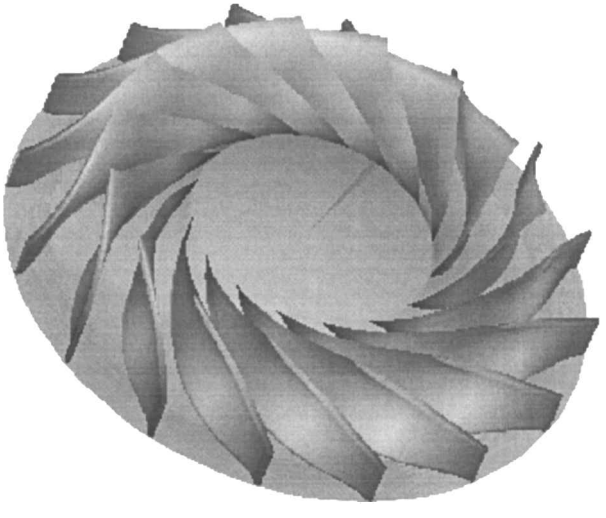

Fig. 11 Solid model for the designed impeller 1.

designed blade. Note that a multigrid type of refinement in control points has been studied in Ref. 28 where three control points were initially used; after one cycle of optimization, the algorithm is refined to seven control points. However, for the present test case no major improvement in loss was achieved by the refinement. The solid model for the designed blade shape generated by the visualization package advanced visual systems (AVS) is displayed in Fig. 11. For this test case a careful examination into the loss variation during the optimization process reveals that the optimal result is not very sensitive to either the level of rear loading at the hub and the loading distribution at the shroud. Despite the discrepancy in the loading distributions, separation is eliminated in both minimizations, and the minimum losses achieved are similar. We can therefore conclude that a rear-loaded hub distribution is the crucial point here in eliminating the separation. Also, we can conclude that three control points are sufficient for this application; consequently the number of unknown design variables remains small.

D. Effect of Optimization Techniques

Here, it is of interest to know whether applying a different optimization technique may change the converged result significantly. In particular, the simplex method and the alternating variables method are compared. The convergence history is shown in Fig. 12, where only the hub distribution is optimized. The same initial guess is used for both methods. The additional starting points for the simplex method are obtained by perturbing this initial guess arbitrarily. From the convergence history the simplex method appears to be more oscillatory, probably because of the flipping action of the simplex. The alternating variables method gives a smoother convergence as the variables are moved gradually away from the initial guess. The optimal loading distributions are given in Fig. 12. Both converged results are rear loaded, and the peak loading is a bit closer to the trailing edge when the alternating variables method is used. Although the loading distributions look quite different, they are roughly comparable because the minimum losses achieved are similar. From this comparison study we can conclude that the optimal result is not very sensitive to the location of peak loading for this test case, as long as the distribution is rear loaded. This conclusion agrees well with the study of parameterization in the preceding section.

E. Effect of Varying Meridional Geometry

In improving the efficiency of a machine, apart from designing the blade geometry sometimes it may be necessary to move the meridional geometry as well. It is suspected that this is essential in multipoint design. As a first step, the hub and shroud meridional geometry are parameterized by spline curves with five control points. The alternating variables method is applied, and the convergence of the optimization is shown in Fig. 13. The circulation distribution is chosen arbitrarily and is fixed throughout. The initial and optimized shapes are depicted in Fig. 14. From the ocillatory nature of the convergence history, it is a sign that the meridional geometry may not be a good design parameter for loss minimization. Some other cost functions should be used instead.

F. Application to the Second Impeller

In general, B-spline curves should give better results than the three segment because of the increased flexibility in the approximation. This is confirmed by this generic compressor design where the

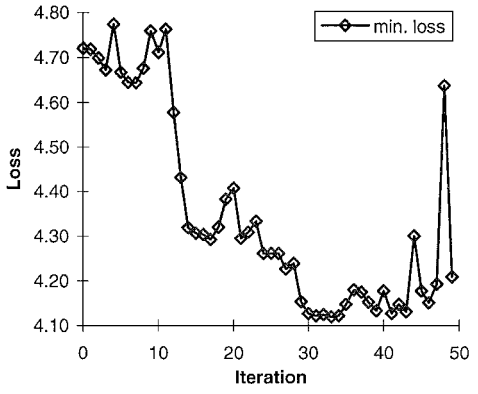

Fig. 13 Convergence history of the meridional geometry optimization.

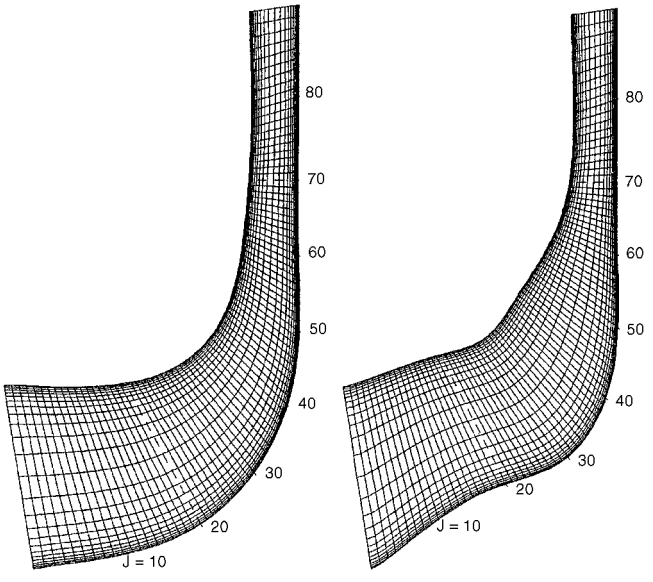

Fig. 14 Initial and optimized meridional geometry.

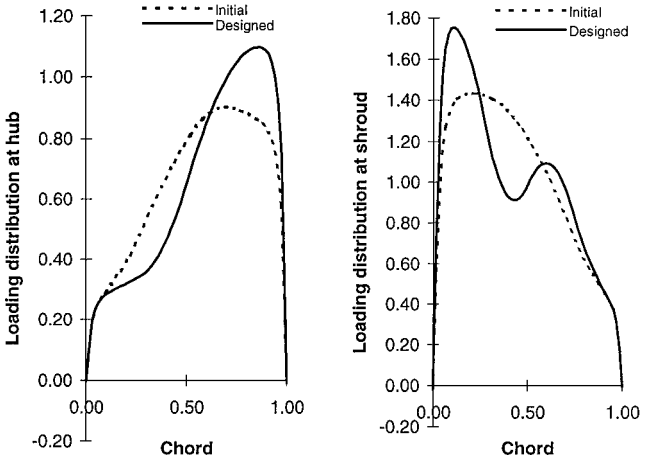

Fig. 15 Comparison of loading distribution.

three-segment technique could not eliminate the separation. After minimizing 1—max(blockage), the comparisons of the initial and the optimal loading distribution are shown in Fig. 15. As seen from the variation of curvatures, the three-segment parameterization would not be able to reproduce this type of variation. The velocity vectors in the blade-to-blade plane near to the shroud for the initial and designed impeller are plotted in Figs. 16 and 17, respectively. Clearly, the separation has been eliminated completely. The solid model for the designed blade shape generated by the visualization package AVS is displayed in Fig. 18.

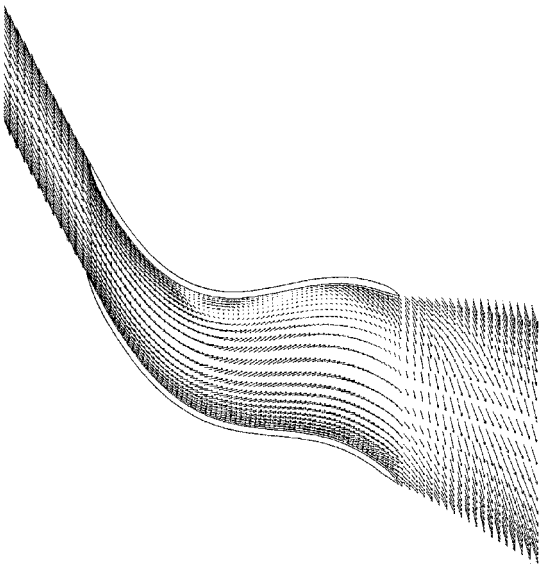

Fig. 16 Initial streamwise velocity vectors near to the shroud.

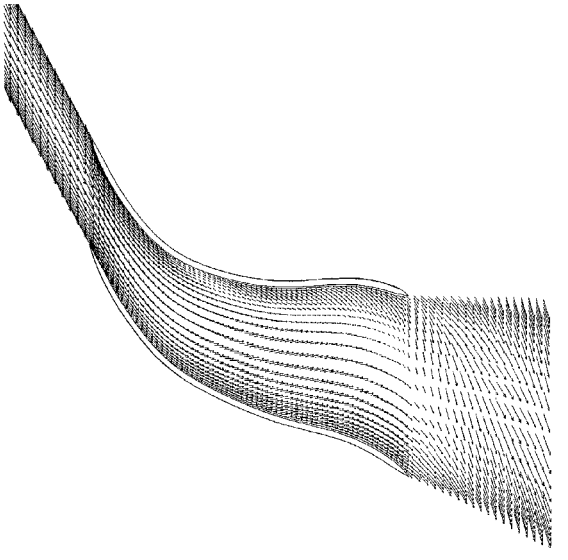

Fig. 17 Optimized streamwise velocity vectors near the shroud.

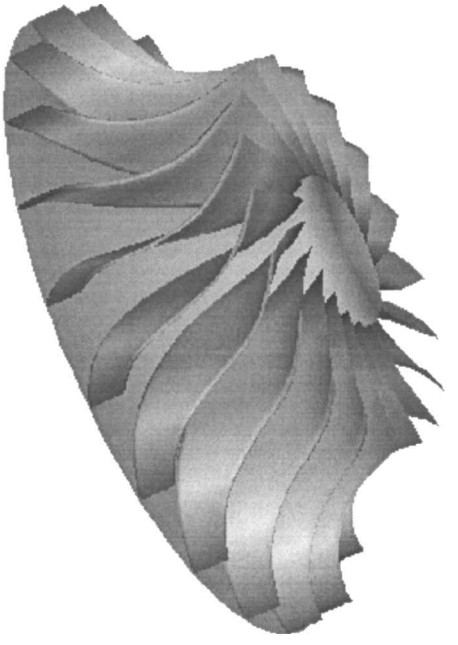

Fig. 18 Solid model for the designed impeller 2.

VII. Conclusions

In this paper an automatic optimization algorithm has been developed. Loss and blockage have been used successfully to suppress flow separations in three-dimensional flowfields. The algorithm has been applied to redesign two generic high specific speed industrial centrifugal compressors. Two methods of parameterizing the circulation distribution have been examined. The first method provides a very smooth loading distribution and is a practical tool for design. The second method based on B-spline curves is a more general method, which has been demonstrated to surpass the first method in certain situations where flow separation cannot be reduced by the first method. In both parameterizations the number of design variables remains fairly small. In choosing the appropriate optimization algorithm the alternating variables method is preferred for the present application because of a smoother convergence history.

The effect of different mesh sizes has been looked at carefully, and the optimized results for both selected coarse mesh and fine mesh have shown a very good agreement, demonstrating that the method is not mesh dependent. The application of the method to redesign two different compressor impeller blades has been very successful. As a first step toward the development of a multipoint design optimization strategy, the optimization of the meridional geometry has also been investigated. Further studies are required to look into the appropriate usage of the meridional geometry in the overall multipoint design process.

Acknowledgments

The authors wish to thank Ebara Research Co., Ltd., of Japan for supporting this work and for their permission to publish this paper. The help of Jeremy See in visualizing the solid models of the designed impellers on AVS is grateful acknowledged.

References

[1]Hicks, R., and Henne, P., "Wing Design by Numerical Optimization," AIAA Paper 77-1247, 1977.

[2]Vanderplaats, G., "An Efficient Algorithm for Numerical Airfoil Optimization," AIAA Paper 79-0079, 1979.

[3]Sadrehaghighi, I., Smith, R., and Tiwari, S., "Grid Sensitivity and Aerodynamic Optimization of Generic Airfoils," *Journal of Aircraft*, Vol. 32, No. 6, 1995, pp. 1234–1239.

[4]Burgreen, G., and Baysal, O., "Aerodynamic Shape Optimization Using Preconditioned Conjugate Gradient Methods," *AIAA Journal*, Vol. 32, No. 11, 1994, pp. 2145–2152.

[5]Burgreen, G., and Baysal, O., "3D Aerodynamic Shape Optimization Using Discrete Sensitivity Analysis," *AIAA Journal*, Vol. 34, No. 9, 1996, pp. 1761–1770.

[6]Baysal, O., Cordero, Y., and Pandya, M., "Improving Discrete-Sensitivity-Based Approach for Practical Design Optimization," *JSME International Conference on Fluid Engineering*, Japanese Society of Mechanical Engineers, Tokyo, July 1997, pp. 417–424.

[7]van Egmond, J., "Numerical Optimization of Target Pressure Distributions for Subsonic and Transonic Airfoil Design," AGARD-CP-463, *Computational Methods for Aerodynamic Design (Inverse) and Optimization*, 1989.

[8]van den Dam, R., van Egmond, J., and Slooff, J., "Optimization of Target Pressure Distributions," AGARD-R-780, *Inverse Methods in Airfoil Design for Aeronautical and Turbomachinery Applications*, 1990.

[9]Drela, M., "Two-Dimensional Transonic Aerodynamic Design and Analysis Using the Euler Equations," Ph.D. Dissertation, Massachusetts Inst. of Technology, Cambridge, MA, 1985.

[10]Leonard, O., and Van den Braembussche, R., 1991, "Design Method for Subsonic and Transonic Cascades with Prescribed Mach Number Distribution," ASME Paper 91-GT-18, 1991.

[11]Zangeneh, M., "A Compressible Three-Dimensional Design Method for Radial and Mixed Flow Turbomachinery Blades," *International Journal for Numerical Methods in Fluids*, Vol. 13, 1991, pp. 599–624.

[12]Aidala, P., Davis, W., and Mason, W., "Smart Aerodynamic Optimization," AIAA Paper 83-1863, 1983.

[13]Trigg, M., Tubby, G., and Sheard, A., "Automatic Genetic Optimization Approach to 2D Blade Profile Design for Steam Turbines," American Society of Mechanical Engineers, Paper 97-GT-392, 1997.

[14]Zangeneh, M., Goto, A., and Takemura, T., "Suppression of Secondary Flows in a Mixed Flow Pump Impeller by Application of Three Dimensional Inverse Design Method. Part 1: Design and Numerical Validation," *Journal of Turbomachinery*, Vol. 118, 1996, pp. 536–551.

[15]Dawes, W., "The Development of a 3D Navier–Stokes Solver for Application to All Types of Turbomachinery," American Society of Mechanical Engineers, Paper 88-GT-70, 1988.

[16]Goto, A., Takemura, T., and Zangeneh, M., "Suppression of Secondary Flows in a Mixed-Flow Pump Impeller by Application of 3D Inverse Design Method: Part 2—Experimental Validation," American Society of Mechanical Engineers, Paper 94-GT-46, June 1994.

[17]Pironneau, O., "Optimal Shape Design for Aerodynamics," *AGARD-FDP-VKI Special Course*, 1994.

[18]Reuther, J., and Jameson, A., "Supersonic Wing and Wing-Body Shape Optimization Using an Adjoint Formulation," *Proceedings of the CFD for Design and Optimization, ASME International Mechanical Engineering Congress and Exposition*, edited by O. Baysal, 1995.

[19]Baysal, O., "Methods for Sensitivity Analysis in Gradient-Based Shape Optimization: A Review," *Proceedings of the American Society of Mechanical Engineers Conference on Fluid Engineering*, 1997.

[20]Bischof, C., Carle, A., Corliss, G., and Griewank, A., "ADIFOR-Generating Derivative Codes from Fortran Programs," *Scientific Programming*, Vol. 1, No. 1, 1992, pp. 11–29.

[21]Fletcher, R., *Practical Methods of Optimization*, Wiley, New York, 1987.

[22]Nelder, J., and Mead, R., "A Simplex Method for Function Minimization," *Computer Journal*, Vol. 7, 1965, pp. 308–313.

[23]Dring, R., "Blockage in Axial Compressors," *Journal of Engineering for Gas Turbines and Power*, Vol. 106, 1984, pp. 712–714.

[24]de Boor, C., *A Practical Guide to Splines, Applied Mathematical Sciences*, Vol. 27, Springer-Verlag, New York, 1978.

[25]Coons, S., "Surface Patches and B-Spline Curves," *Computer Aided Geometric Design*, edited by R. Barnhill and R. Riesenfeld, 1974, pp. 1–16.

[26]Press, W., et al., *Numerical Recipes in Fortran: The Art of Scientific Computing*, 2nd ed., Cambridge Univ. Press, 1992.

[27]Powell, M., "On Search Directions for Minimization Algorithms," *Mathematical Programming*, Vol. 4, 1973, pp. 193–201.

[28]Yiu, K., and Zangeneh, M., "A 3D Automatic Optimization Strategy for Design of Centrifugal Compressor Impeller Blades," American Society of Mechanical Engineers, Paper 98-GT-128, June 1998.